Predator and prey dynamics with Beddington-DeAngelis functional response with in kinesis model

Tahani Al-Karkhi
School of Mathematics
Statistic and Actuarial Science
University of Essex
Wivenhoe Park, Colchester CO4 3SQ
United Kingdom
tasalk@essex.ac.uk

Nardun Gobukoglu
School of Mathematics and Computer Science
University of Wolverhampton
Wolverhampton, WV1 1LY
United Kingdom

Abstract. In mathematical ecology, the study of interactions that are reactive-diffusive in nature between different species and their relevant systems has been researched extensively. However, there is still room for contribution on this rich topic. Therefore, we study a spatial-temporal prey-predator model which includes kinesis terms representing plankton dynamics under info-chemical mediated trophic interactions. The Beddington-DeAngelis functional response is coupled with a simplified two species approach within the model to describe the grazing pressure of zooplankton (M) on phytoplankton (P).This pressure is controlled through an external info-chemical (C). The mutual interference by predators within the ecosystem is implemented through the Beddington-DeAngelis functional response, a distinctive feature of this response type. This feature is utilized in this study to indicate the effect of changes in prey density in relation to predator density. In our model, a stability analysis is performed between the two aforementioned species to provide a system dynamics comparison. The critical conditions for kinesis are derived on the basis that increases in the reproduction coefficient decrease the diffusion. This means that species prefer to stay in good conditions to facilitate the reproduction process, but are likely to escape in bad conditions. The kinesis terms within our Phytoplankton-Zooplankton model impact factors such as survival and traveling wave behavior. Numerical experiments are performed in this work to examine the traveling waves and the monotonic dependence of the reproduction coefficient in the species population. Moreover, the possible benefits of purposeful kinesis are demonstrated.

Keywords: bifurcation analysis, stability analysis, predator-prey dynamics, plankton model, reaction-diffusion with kinesis model, travelling waves.

MSC 2020: 35A24

1. Introduction

Phytoplankton are the primary source of carbon dioxide transfer to the ocean and capture carbon dioxide through the process of photosynthesis. Carbon capture, and modelling processes involved, has recently become a topic of increasing interest, given its potential role in countering global warming, although little novel mathematical research into this aspect has been published in recent years. We wanted to improve the modelling of the interactions between a particular group of phytoplankton and its main predator. Phytoplankton need light for photosynthesis. This limits their viable depth to less than 200m [27]. The vertical distribution of phytoplankton is highly heterogeneous, but empirical research has shown that profiles of certain chemicals (info-chemicals), for instance dimethyl sulfide (DMS), closely resemble chlorophyll maxima (i.e. clusters of phytoplankton) as seen in [28]. Predators of plankton (e.g. Copepods) are known to travel vertically to follow prey distribution. This suggests that Copepods may use vertical gradients of info-chemicals to locate prey and remain within their profitable foraging zones. Lewis [52] developed a non-spatial model involving Copepods. Further investigation showed that small increases in the ability of Copepods to sense info-chemicals could increase their longevity in the system, and hence increased sensitivity to info-chemicals can be an evolutionarily advantageous a strategy for these predators. The phenomenon of vertically migrating zooplankton has been studied by many (e.g., [29], [30], [31], [65]), including a spatial heterogeneity which lead to the development of reaction-advection-diffusion models. The Beddington DeAngelis functional response is an essential tool in the field of plankton modelling. Although it is similar to responses such as the Holling type II functional response, it includes a term that accounts for mutual interference by predators. This allows for the prediction of predators per capita feeding rates on the prey, as well as providing better descriptions of predator-prey abundances and their relation to predator feeding activity within their respective predator-prey systems. In plankton models, the Beddington DeAngelis functional response can be used to perform a detailed mathematical analysis of the intra-species competition among predators [21]. Many ecologists have proposed the prey dependent predator-prey model, based on the assumption that the predators rate of prey capture is independent of prey density. However, some biologists disagree with that in many instances, particularly when predators must search for food and thus must share or start competing for food, the predator prey models deliver results should really be predator dependent. The Beddington DeAngelis type functional response outperformed the others in several circumstances. The functional response of a predator is the rate at which it consumes prey as a function of food density. Understanding the underlying dynamic relationships between prey and predator in the Beddington DeAngelis model is crucial for the description of ecosystem dynamics. [21, 26] implemented the effect of this functional response to describe mutual interference by predators within their predatorprey ecosystem

model. Later this approach was used to highlight the effect of changes in prey density on the predator density attached per unit time in Sarwardi [25]. [58] and [48] introduced the classical PDE model which defines population dispersal, and is used to model kinesis, as can be observed in [42]. For those kinesis models, the diffusion is dependent on only localized information rather than including non-localized information. The local information, which is to be considered in cases such as taxis movement. A connection between the reproduction rate and diffusion coefficient has been established in which the reproduction coefficient can be presented as Darwinian Fitness; increase in migration should increase Darwinian Fitness [47], [54], and [41]. In this work, we aim to explore a predator-prey diffusion model of plankton with kinesis using partial differential equations (PDEs). [64] analytically explained the random population dispersal mechanics for living organisms by introducing the diffusion law, enabling an understanding of the spatial distribution of population density in linear and two-dimensional forms. Over the years, many scientists have studied diffusion to model biological, chemical, and physical processes. In particular, Alan Turing determined the causes of d-patterns in a variety of non-equilibrium situations when dealing with reaction-diffusion [4]. The classical predator-prey model was defined by Lotka and Volterra in 1920. In n our study, we investigate five key aspects related to the kinesis-diffusion terms, which provide a parameterisation of small-scale distribution. These terms account for horizontal movement in two dimensions, primarily influenced by the circular distribution and flows observed in plankton. Here's an overview of the sections covered in our study:

- General Description and Mathematical Model: The first section provides an introduction and outlines the mathematical model used in our research.
- Equilibrium Location and Analysis: The second section focuses on the location and analysis of equilibrium points within the model.
- Time-Series Behavior: Section three delves into the time-series behavior of the system, examining its dynamic evolution over time.
- Bifurcation Behavior at Different Carrying Capacity Levels: In the fourth section, we explore how the system's behavior changes at various carrying capacity levels, particularly focusing on bifurcation phenomena.
- Hydra Effect of Both Predator and Prey: Section five discusses the "hydra effect" observed in both predator and prey populations and its implications for the ecosystem.
- Analysis of Kinesis in the Reaction-Diffusion System: The sixth section provides an in-depth analysis of kinesis within the reaction-diffusion system and its impact on the overall equilibrium.
- Discussion of Findings and Conclusion: The final section offers a comprehensive discussion of our research findings. We conclude by discussing how

a small growth rate can lead to reduced phytoplankton density and potentially destabilize the model. Additionally, we explore the role of rapid responses to increases in fast-growing prey, which can contribute to the emergence of limit cycles in the dynamical system.

2. Mathematical model

The core goal of our work is to analyze the qualitative behavior of two microorganism species (phytoplankton, grazing zooplankton) interacting on two trophic levels exposed to a predator (meso-zooplankton copepod) and to examine the interaction between this trophic. The analysis will focus on a comparison between the latest obtained results and the current available results in an attempt to understand the main difference among two different functional response types in the predator-prey model and to illustrate how grazing induced by Dimethyl sulphide has a stabilizing effect on the modelled system.

2.1 General model and description

The model used is described using PDEs which include a horizontal diffusion term as shown below:

$$\frac{\partial P}{\partial t} = F_\Delta(P,M) := D_P \frac{\partial^2 P}{\partial x^2} + rP\left(1 - \frac{P}{K}\right) - \frac{aPM}{EM + P + b}, \tag{1}$$

$$\frac{\partial M}{\partial t} = G_\Delta(P,M) := D_M \frac{\partial^2 M}{\partial x^2} + \frac{\gamma aPM}{EM + P + b} - mM - \nu \frac{aPM^2}{EM + P + b}, \tag{2}$$

In the given model (Eq. 2), P and M represent the densities of phytoplankton and zooplankton within a closed homogeneous system. Similar to the approach taken by [52], the model assumes logistic growth for phytoplankton, characterized by an intrinsic growth rate denoted as r and a carrying capacity represented by K. This carrying capacity reflects the limits imposed by nutrient availability and self-shading effects on phytoplankton growth. Zooplankton in this model feed on phytoplankton based on the Beddington DeAngelis functional response, a mathematical framework used to describe predator-prey interactions. This functional response is employed to provide more detailed insights into predator-prey dynamics and how they influence predator feeding behavior. The Beddington DeAngelis functional response has been used in various ecological studies to elucidate the impact of changes in prey density on predator density over time. For instance, [26] applied this concept to illustrate mutual interference among predators in an ecosystem, while [25] examined how alterations in prey density affect the per capita feeding rates of predators. Haque [21] demonstrated that the Beddington DeAngelis functional response is suitable for conducting a comprehensive mathematical analysis of intra-specific competition among predators. This response model reflects the saturation of grazing rates at higher phytoplankton densities, with phytoplankton biomass converted into

zooplankton biomass with an efficiency factor denoted as γ. Additionally, the parameter E accounts for predator interference within the system. The parameter m represents zooplankton mortality, primarily caused by copepods, but it also considers mortality due to processes such as sinking and additional predation by other zooplankton or higher trophic levels. The parameter ν has a slightly different interpretation compared to its usage in [1] and [52]. It reflects an increase in copepod predation on zooplankton in response to the immediate release of info-chemicals when phytoplankton are grazed. Thus, ν can represent both heightened copepod sensitivity and response to chemical cues and improved copepod search efficiency at higher chemical concentrations. Importantly, copepods and info-chemicals are not explicitly modeled as variables but are incorporated into the system through the interaction term involving ν. The parameters a and b respectively represent the clearance rate of zooplankton at low food densities and its half-saturation density. Typical parameter values are summarized in Table(2.1). Notably, this model differs from the one presented by [1] and [52] primarily in the choice of functional response type. Additionally, Laplacian terms, represented by D_P and D_M, are included in the model, reflecting the diffusion of phytoplankton and zooplankton, respectively, with strengths defined as D_P and D_M. These terms account for the spatial movement of these populations, and this aspect of the model is consistent with the previous work in [1].

Table 1: Model Parameter Values

Parameter	Value	Unit	Source
r	$0-5$	day^{-1}	[8]
K	$0-1000$	$\mu g\ C\ I^{-1}$	[9, 10]
a	0.3	$\mu g\ CI^{-1}\ \text{day}^{-1}$	[11, 12]
b	0.05	$\mu g\ C\ I^{-1}$	[11, 12]
γ	0.3	day^{-1}	[13]
m	0.3	day^{-1}	
ν	$0.01-0.2$	day^{-1}	
E	0.2	day^{-1}	

2.2 Location of equilibria

The equilibrium points $P(t) = P_e$ and $M(t) = M_e$ ofEq.(1-2), corresponding to $dP/dt = dM/dt = 0$, can be shown to include the trivial state $(P_{e,0}, M_{e,0}) =$

$(0,0)$, the zooplankton-free equilibrium $(P_{e,mf}, M_{e,mf}) = (K, 0)$, and the co-existence state that satisfies the polynomial.

$$(3)\quad r\nu P_e^3+(-E\gamma r-K\nu r+\nu br)P_e^2+(E\gamma Kr-K\nu 180br-\gamma Ka+K*m)P_e-mkb$$

and

$$(4)\qquad M_e=\gamma r\frac{\begin{array}{c}\nu r P_e^3+(-E\gamma r-K\nu r\\ +\nu br)P_e^2+(E\gamma 187Kr-K\nu br-\gamma Ka+Km)\end{array}}{ak}$$

In general, Eq.(3) will have three roots. Following [6], they are given by

$$(5)\qquad \begin{array}{l}P_{e,j+1}=\dfrac{Kb-1}{3b}\\ +\dfrac{2}{3b}\sqrt{(KEGb-1)^2-\dfrac{3EGK}{r\nu}(\gamma a-mb-\nu r)}\cos\left(\dfrac{\theta+2j\pi}{3}\right),\ j=0,1,2,\end{array}$$

where $\theta=\cos^{-1}\left(\frac{y_N}{h}\right)$,

$$y_N=-r\nu\frac{(Kb-1)^3}{9b^2}+\frac{r\nu(Kb-1)^2}{27b^2}+\frac{K(\gamma a-mEGK-\nu r)(Kb-1)}{3b}-mK,$$

and

$$h=\frac{2\nu rb}{27}\left(\frac{(-EGr-K\nu r+\nu br)^2-3\nu r(EGKr-K\nu br-GKs+Km)}{\nu^2r^2}\right)^{\frac{3}{2}}.$$

The phenomenon of two roots merging into one occurs when the condition $y_N^2 = h^2$ is satisfied, leading to the emergence of a complex-valued root. This cubic nature of the solution, as described byEq.(5), is clearly depicted in Fig. 2 for the case where $K = 120$, $r = 1.5$, and other parameters maintain values as specified in Table. 2.1. The presence and number of coexistence equilibria in the system are notably influenced by the parameter values of K and ν. For instance, when $K = 70$, as illustrated in Fig. (2) (c), there exists only a single real root of Eq. (5) for all values of ν. However, when $K \approx 70.78$, a significant event known as a saddle-saddle bifurcation occurs. This corresponds to the moment when the two saddle node bifurcation points converge or collide.

3. Analysis of equilibrium points in the non-spatial model

In this section, we delve into the dynamics of plankton populations and engage in a discussion centered on our comprehension of the non-spatial interactions, often referred to as local interactions, within the marine ecosystem. Our focus revolves around examining the complex interactions among multiple trophic levels that take place in aquatic environments. To accomplish this, we employ

a reaction-diffusion model as a tool for our investigation.

$$\begin{pmatrix} P(t) \\ M(t) \end{pmatrix} = \begin{pmatrix} P_e \\ M_e \end{pmatrix} + \begin{pmatrix} \epsilon_1 \\ \epsilon_2 \end{pmatrix} e^{\lambda t}. \tag{6}$$

FromEq.(6), a uniform solution is said to be linearly stable when $\lambda \leq 0$ and unstable otherwise. Substituting (6) into (2) and linearising about $\epsilon_1 = \epsilon_2 = 0$, we obtain the linear eigenvalue problem

$$\lambda \begin{pmatrix} \epsilon_1 \\ \epsilon_2 \end{pmatrix} = \begin{pmatrix} a_{11} & a_{12} \\ a_{21} & a_{22} \end{pmatrix} \begin{pmatrix} \epsilon_1 \\ \epsilon_2 \end{pmatrix}, \tag{7}$$

where

$$\begin{aligned} a_{11} &= r(1 - \frac{2rP_e}{K}) - \frac{abM_e + EaM_e^2}{(b + P_e + EM)}, \\ a_{12} &= -aP_e \frac{2EM_e + P_e + b}{(EM_e + P_e + b)}, \\ a_{21} &= 2\frac{(EM_e + b)}{(EM_e + P_e + b)^2}, \\ a_{22} &= -m - \frac{(P_e+b)\gamma aP_e}{(EM_e+P_e+b)} - \frac{EM_e^2\nu aP_e - 2M_e\nu aP_e^2 - 2M_eb\nu aP_e}{(EM_e + P_e + b)}. \end{aligned} \tag{8}$$

The eigenvalues can then be readily obtained

$$\lambda_{\pm} = \frac{1}{2}\left[a_{11} + a_{22} \pm \sqrt{(a_{11} - a_{22})^2 + 4a_{12}a_{21}}\right]. \tag{9}$$

The model in Eq.(2) posses three different equilibria; Table. (2) provides a description of the stability of each equilibria. The mathematical model presented in Eq.(2) in the absence of diffusion is firstly considered by us, i.e. $D_P = D_M = 0$, which is similar to the first approach by [1]. The summary of the equilibrium stability is given in Table. (2): Note that Eq.(3) is a cubic polynomial, and all its

Table 2: Biologically Relevant Possible Equilibria of the System given by Eq. (2)

Equilibrium	Definition	Value in parametrized system	Description	Hyperbolic Eigenvalues
E_0	(P_e, M_e)	$(0, 0)$	Trivial (extinct)	stable node point
E_1	(P_e, M_e)	$(K, 0)$	The carrying capacity of phytoplankton	stable node
E_3	(P_e, M_e)	Eq.3 and 4	equilibrium Coexistence point	different stability behaviours

roots can be found by using **Cardan's method** [6]. Consequently, the obtained roots are utilized to determine the roots of the second species in Eq.(4). The stability of the coexistence point determines the behavior of the system given in Eq.(2).

4. Numerical exploration of the model

his section of the study will delve into the impact of varying parameters such as K, ν, and r on the stability of the system. In the subsequent subsection, we will introduce and define these parameters more explicitly, elucidating the specific ranges and values that could result in distinct system behaviors. This will be detailed further in the bifurcation and stability analysis section. Moreover, we will present the system's phase portrait and the equilibrium values associated with each intersection of the nullclines. The plane is inherently divided by several nullclines into distinct regions, each of which provides information about how the system behaves at different points within the plane [32]. These regions and their descriptions collectively offer a comprehensive understanding of how the system changes across various points in the plane.

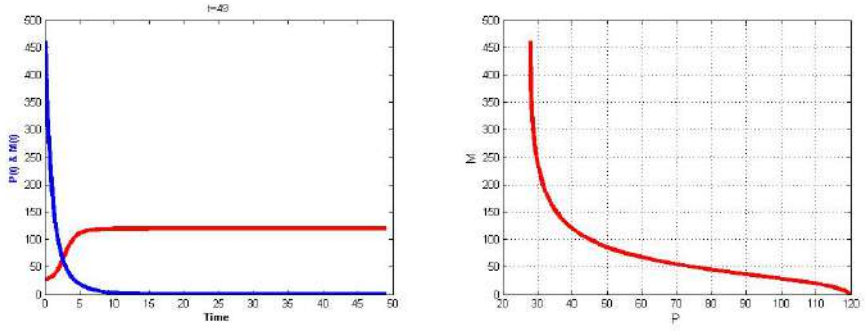

(a) (b)

Figure 1: The time series behavior and phase portrait of the system are representative of the parameter setting where $\nu = 0.145$.

4.1 Bifurcation analysis of the phytoplankton-zooplankton model across various carrying capacity (K) and info-chemical (ν) levels

It is evident that the carrying capacity plays a crucial role in determining the maximum population density for plankton in each model [1]. In this work, an interesting finding relates the carrying capacity to the info-chemical parameter DMS, effectively introducing two control parameters instead of one. Fig. (2) illustrates four cases for different values of the carrying capacity (K), while keeping all other parameters fixed at the values provided in Table. (2.1). In Fig. (2(a)), (2(b)), and (2(c)), the system exhibits hysteresis behavior. Specifically, when $K = 1000$, there is an overlapping Hopf bifurcation at $\nu = 0.036$. Initially, as the info-chemical interaction parameter ν decreases from 1000 to 70, a supercritical Hopf bifurcation (Hp) occurs. During this phase, the system transitions from a stable limit cycle around the unstable coexistence state to a single stable coexistence state. Subsequently, a saddle-node bifurcation results in a region

with bi-stability, where two stable coexistence states coexist alongside one unstable (saddle) coexistence state. The local stability of the stable equilibria shifts from a focus to a node, and the eigenvalues change from complex to real values. At this point, the system acquires the monotonicity property, meaning that the solution approaches a stable equilibrium in a monotonous manner, referred to as over-damped oscillations [14]. Finally, a second saddle-node bifurcation takes place, leaving only the larger stable coexistence state in the system. This outcome aligns with the findings of [1] and has been interpreted by [52] as the threshold at which persistent phytoplankton bloom formation becomes possible. In this context, persistent bloom formation implies that P_e (the phytoplankton equilibrium point) remains stable and approaches K. In Fig. (2(d)), the system exhibits less hysteresis behavior, with only one stable focus root type across all ν values. This variation is attributed to the influence of DMS on the predation of grazers. The bifurcation analysis for the behavior of zooplankton was con-

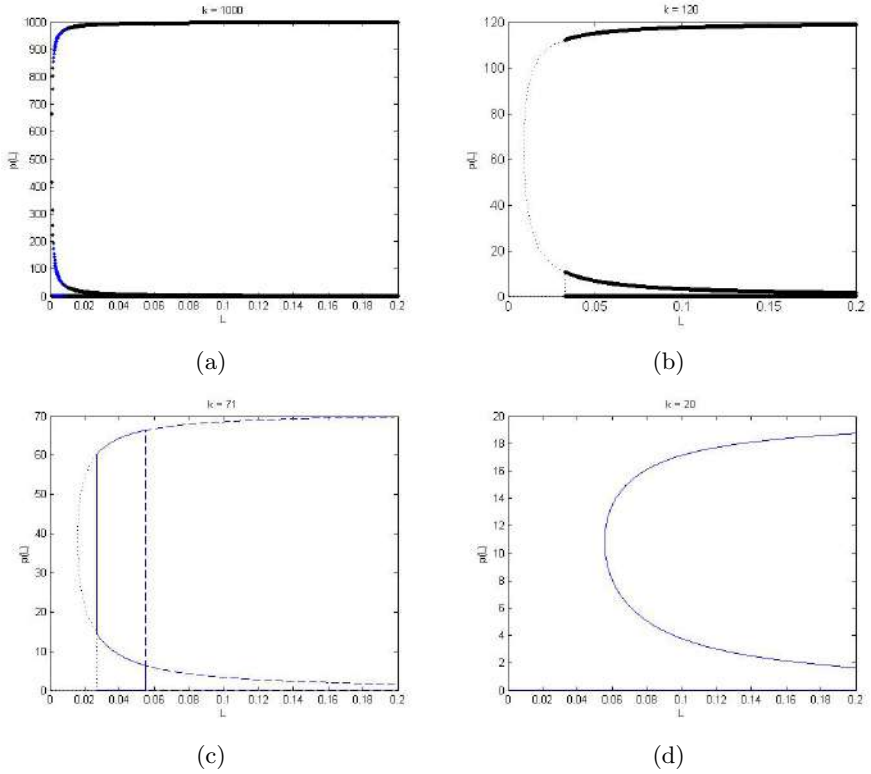

(a) (b)

(c) (d)

Figure 2: Bifurcation diagram correspond to different values of K in prey (phytoplankton) analysed system

ducted while keeping all other parameters fixed at the values specified in Table 21.1. In Fig. (3(a)), there is an overlap in the bifurcation behavior, specifically, a Hopf bifurcation occurs within the same range, with a value of approximately

0.036. Additionally, the two limit points correspond to a saddle-node bifurcation. In the case of Fig. (3(b)), both Hopf and saddle-node bifurcations can be observed. Fig. (3(c)) demonstrates that the system undergoes a Hopf bifurcation at $\nu = 0.01934$, after which the system's roots indicate a stable sink/node behavior. Lastly, in Fig. (3(d)), which examines the influence of DMS on grazer predation, the equilibrium type remains a 'stable focus' for all values of ν. The

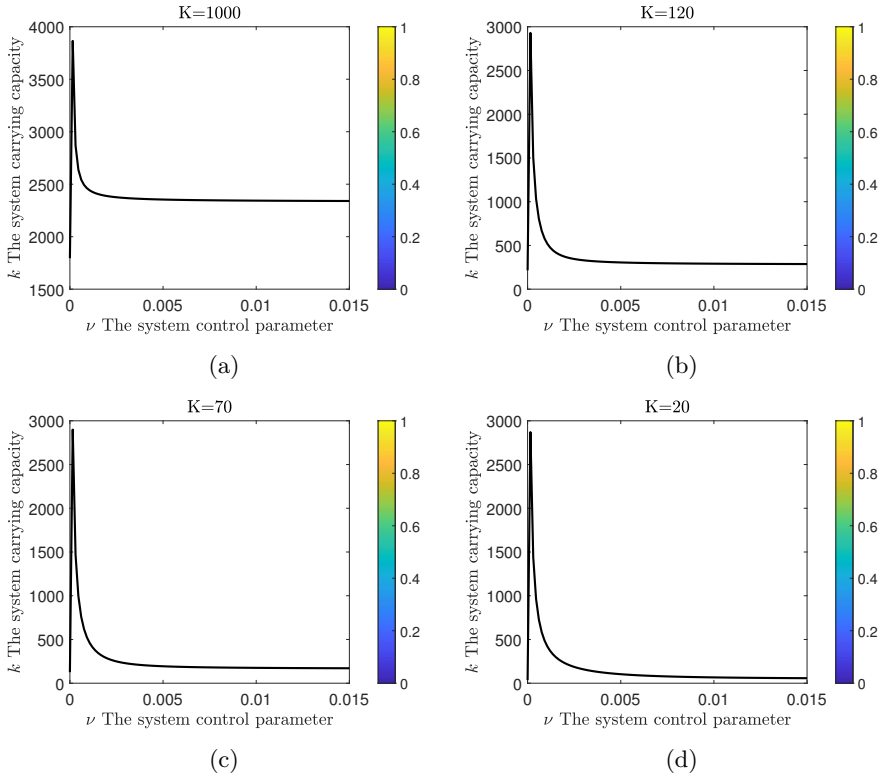

Figure 3: Bifurcation Diagram corresponding to Different Values of K in Predator (zooplankton).

model described inEq. (2) demonstrates the presence of a limit cycle for various values of K, as depicted in Figures 2 and 3. These findings align with the expected essential characteristics of the system.

4.2 Phytoplankton and zooplankton heat-maps

A phytoplankton bloom is characterized by a significant increase in the concentration of phytoplankton in a specific area. This phenomenon typically occurs when environmental conditions are favorable for enhanced reproduction, such as a continuous nutrient supply and suitable survival conditions. The formation of a phytoplankton bloom can occur within a specific range of parameter combina-

tions involving K and ν. When copepod predation on zooplankton intensifies, it reduces the grazing pressure on phytoplankton, creating conditions conducive to bloom formation. The solution to Eq. (3) provides the roots for the saddle-node bifurcation and identifies the bifurcation position. It's essential to note that the region between the area with one real root and the area with three real and distinct roots is defined by satisfying Cardan's third condition, namely $y_N^2 = h^2$, effectively separating these regions as outlined in Eq. (3). Phytoplankton blooms can have a lasting impact on ecosystems [22, 23], and such occurrences have been referred to as the "hydra effect." The outcomes displayed in Fig. (4) depict the maximum population density of phytoplankton concerning variations in the carrying capacity. Generally, a phytoplankton bloom is characterized by a rapid proliferation of phytoplankton populations. These blooms tend to occur when there's an abundance of sunlight and nutrients available, creating favorable conditions for plant growth and reproduction. In such scenarios, the plants proliferate to the point where they become widespread, altering the water's color in which they reside [24]. Fig. (4) investigates two independent parameters: the carrying capacity and the infochemical concentration, determined using the polynomial in Eq. (3). This analysis suggests the potential occurrence of a phytoplankton bloom. A small, dark region on the left side of the saddle-node curves depicted in Fig. (2) (a) corresponds to a low phytoplankton population. Fig. (4) (a) readily illustrates the low values of P_e (the phytoplankton equilibrium point) for various combinations of K and ν, while the area to the right of the curve indicates higher phytoplankton populations, signifying the potential for a phytoplankton bloom.

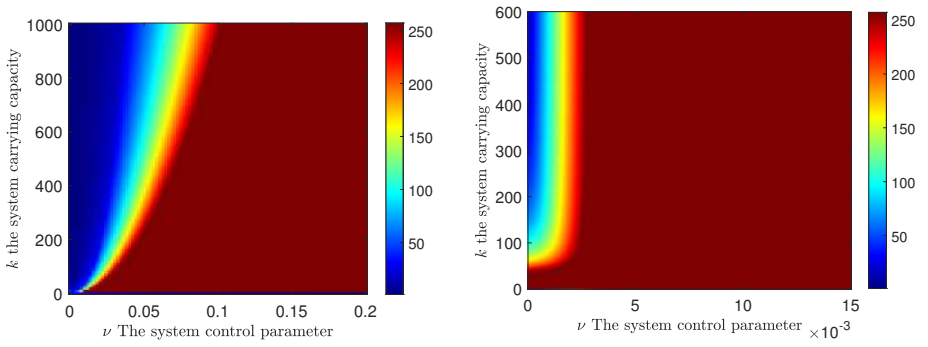

(a) (b)

Figure 4: The heatmap in panel (a) pertains to the population of phytoplankton when subjected to the grazing pressure exerted by zooplankton. Panel (b) illustrates the population of zooplankton.

5. Analysis of predator-prey diffusion model with kinesis

In this section, we analyse the predator-prey diffusion model with kinesis that was first defined by [42] as follows:

$$\boxed{\partial_t u_i = D_{0i}\nabla \cdot \left(e^{-\alpha_i r_i(u_1,\ldots,u_k,s)}\nabla u_i\right) + r_i(u_1,\ldots,u_k,s)u_i,} \tag{10}$$

where:

u_i is the ith species-population density,

s is the abiotic characteristics of the living conditions,

r_i is the reproduction coefficient,

$D_{0i} > 0$ is the equilibrium diffusion coefficient which is defined when the reproduction coefficient is 0,

$\alpha_i > 0$ defines the relation between the diffusion coefficient on the reproduction coefficient.

We can define $D_i = D_{0i}e^{-\alpha r_i}$ as the diffusion depending on reproduction coefficient. It has been shown in [42] that, the diffusion depends on well-being and it can be measured by the reproduction coefficient. In this section, we will present the new predator-prey plankton model with kinesis and compare the results with basic Kinesis model. The PDE model for population with constant diffusion coefficient without kinesis has been presented by (Kolmogorov, Petrovsky and Piskunov, 1937) (KPP) [50] as follows:

$$\partial_t u(t,x) = D\nabla^2 u(t,x) + (1-u(t,x))u(t,x). \tag{11}$$

We will consider the predator-prey model presented Eq.(2) to define plankton-kinesis model as in Eq. (**??**).

$$\begin{aligned}
&\frac{\partial P}{\partial t} = F_\Delta(P,M) := D_P\nabla\cdot\left(e^{-\alpha(r\left(1-\frac{P}{K}\right)-\frac{aM}{EM+P+b})}\nabla P\right)\\
&+ rP\left(1-\frac{P}{K}\right) - \frac{aPM}{EM+P+b},\\
&\frac{\partial M}{\partial t} = G_\Delta(P,M) := D_M\nabla\cdot\left(e^{-\alpha(\frac{\gamma aP}{EM+P+b}-m-\nu\frac{aPM}{EM+P+b})}\nabla M\right)\\
&+ \frac{\gamma aPM}{EM+P+b} - mM - \nu\frac{aPM^2}{EM+P+b},
\end{aligned} \tag{12}$$

Figure 5 indicates that kinesis movement has no effect on the predator model. On the contrary, kinesis does affect prey population. Kinesis movement prevents extinction of prey population for a time. The MATLAB [59] function was used in this study to solve the one-dimensional system of PDE. The space interval

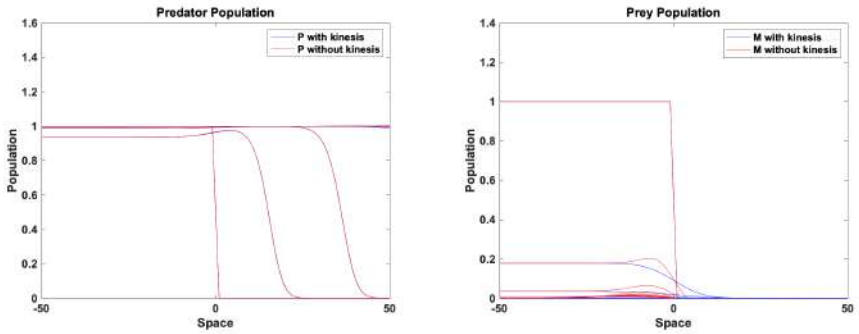

(a) a (b) b

Figure 5: Predator-prey mobility under the effect of kinesis model.

was selected to be $[-50, 50]$ with zero-flux boundary conditions and with the initial conditions given below:

$$P(x,0) = P_e + \sigma\cos(wP), M(x,0) = M_e + \sigma\sin(wM) \tag{13}$$

The values of the constants are: $D = 1$, $\alpha = 1$.

In Fig.6 gives an account of the population size differences between the population with and without kinesis over time. Due to predatory causes, the prey population faces extinction within a small amount of time. The prey population without kinesis survives better than the one with kinesisin time 10, after in a while ($time20$), the population tends to survive better with kinesis movement over time. There is no time difference in the time profile of predator population with and without kinesis.Thus, there will be no difference in population size if we were to compare P with kinesis and without kinesis. Alternatively, kinesis decreases the size of prey population P with kinesis. This suggests that, initially, kinesis is not beneficial for the prey population in space. However, it starts to become beneficial and the population survives when the prey population without kinesis is dying (see Fig.6). In Fig.7, the travelling wave behaviour can be seen in the predator population in space. Initially, the predator population decreases in time and then it starts to increase and stabilizes over time. The kinesis movement affects prey population in a negative manner; it leades to population death in both conditions exponentially, and to an accelerated death in kinesis condition.

At the time 20, it can be clearly seen in space that both predator and prey population exhibit travelling wave behaviour (Fig.8). Figure 9 illustrates how the predator population dies over time in the spatial distribution, yet predators survive for a long time. M with kinesis decreases a faster, but survives better over time.

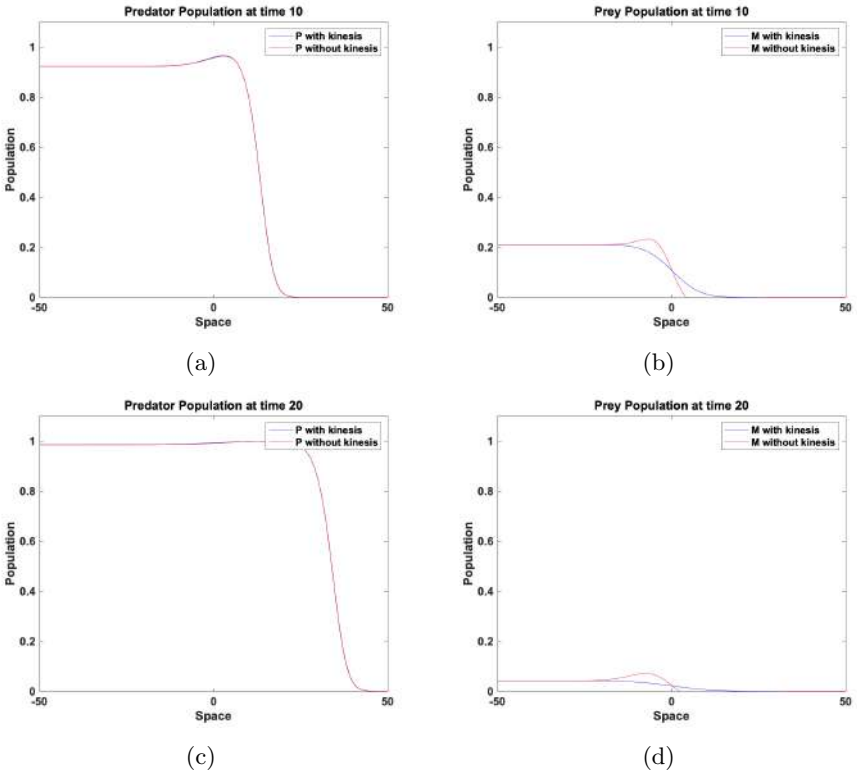

Figure 6: Prey mobility without and with kinesis.

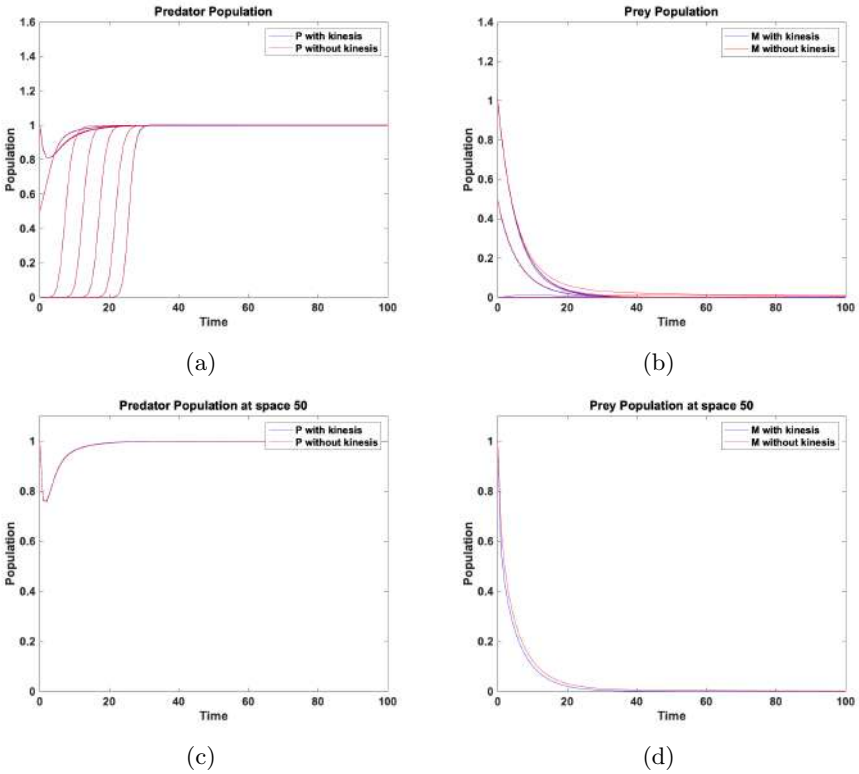

Figure 7: Predator mobility without and with kinesis.

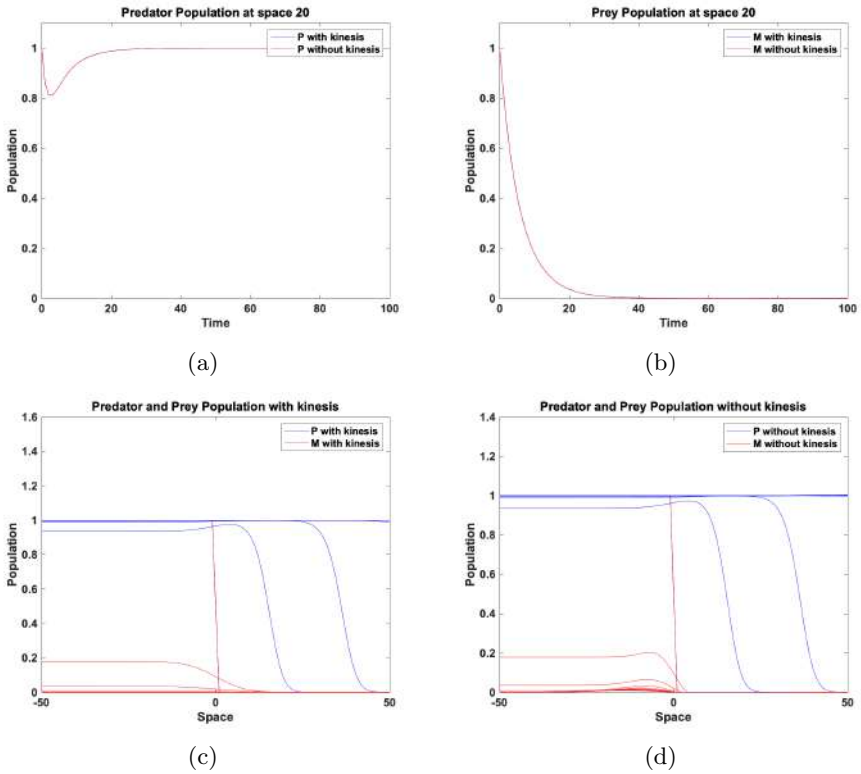

(a) (b)

(c) (d)

Figure 8: Predator and prey population without and with kinesis movement

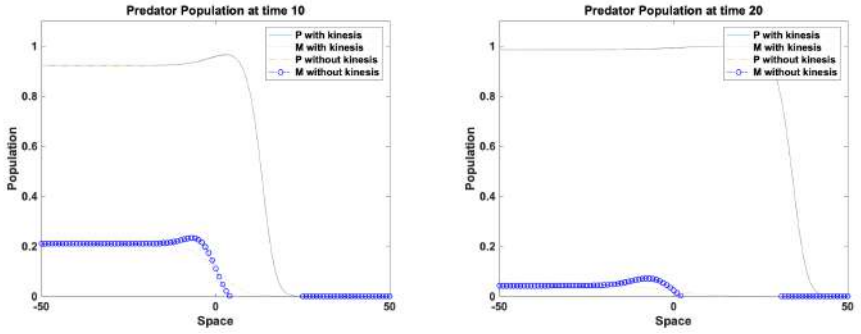

(a) (b)

Figure 9: Predator prey population without and with kinesis movement

6. Conclusion

We gained insight into the behavior of the system described by equations Eqs. (2) by conducting a mathematical analysis involving phase plane investigations, stability assessments, and bifurcation examinations. Since we assume a uniform environment, we opted to employ the Beddington-DeAngelis functional response. This choice was motivated by the fact that it exhibits a broader spectrum of dynamic behaviors, as documented in previous studies [21]. This aligns with existing literature, which generally favors the utilization of the Beddington-DeAngelis functional response, particularly when examining interactions between two species, such as microzooplankton grazers like Oxyrrhis marina [17], [18]. In our numerical approach, we investigated the impact of the control parameter ν on the system's qualitative behavior. This investigation was made possible through the use of the phase plane tool, as demonstrated in Figs. 1(a) and 1(b). To illustrate, when setting ν to zero, we effectively transform the system into the Rosenzweig-MacArthur model [2]. In this scenario, the system becomes unstable, and we observe periodic cycles in the microzooplankton and phytoplankton population densities. This phenomenon is akin to the predator-prey interactions explored by [19] and [20], where the system exhibits a stable equilibrium, but the solution trajectories undergo substantial oscillations before returning to that equilibrium. As the control parameter increases, it leads to various stability scenarios, as depicted in the bifurcation diagram (Fig. 2) and its specific instances illustrated in Figs. 2(a), 2(b), and 2(c). This variation elucidates how infochemical signaling serves as a mechanism for enhancing copepod predation on microzooplankton. This article provides a comprehensive analysis of the system's behavior, including an examination of the location, number, and type of roots, determined using Cardan's method. Notably, this analysis helps identify crucial system parameters, particularly when $K = 70.34$, marking the point of a cusp bifurcation, where two equilibrium points merge and vanish in a saddle-node bifurcation [16]. The investigation extends to the (ν, K) plane, uncovering the phenomenon of a microzooplankton "hydra effect" on copepod predation. Additionally, the model allows for predictions regarding the occurrence and locations of phytoplankton blooms, as depicted in Fig. 3. An examination of Fig. 2 reveals that the system exhibits five distinct stability states, all of which are elaborated upon in Section 4. The text also discusses the implications of altering the growth rate and phytoplankton carrying capacity on phytoplankton behaviors, as illustrated in Figs. 4(a) and 4(b). It emphasizes how lower growth rates can shift the model's stability towards its current configuration. Furthermore, a relationship between both K and ν is identified, suggesting that both species can thrive in environments abundant with nutrients, as shown in Fig. 2. This outcome exemplifies the "hydra effect" within the predator-prey model, as mentioned in [15]. However, the primary objective of this article is to establish coherence between the model presented in Eq. 2 and the one examined in [1], both analytically and numerically.

The concept of population dispersion within a partial differential equation (PDE) model was initially introduced by [58] and further developed by [48]. The diffusion model, incorporating kinesis, has been the subject of prior research by [42]. In this context, kinesis movement influences the reproduction rate, and an interesting relationship emerges between the diffusion coefficient and the reproduction coefficient. Specifically, when reproduction rates increase over time, the diffusion coefficient decreases in contrast. This phenomenon aligns with the overarching principle that populations inherently strive for prolonged existence. Conversely, when population reproduction declines, indicating a population decline, individuals seek to disperse through kinesis movement. This behavior is driven by the imperative to escape unfavorable conditions and pursue more favorable ones. This notion of population dynamics can be likened to the concept of Darwinian fitness, as proposed by [47], [54], and [41]. According to this perspective, migration is a strategy employed to enhance Darwinian fitness, ultimately ensuring the population's survival. Consequently, populations tend to remain within beneficial areas while actively avoiding perilous conditions. To encapsulate our model's discoveries, we can outline them as follows:

- The eigenvalue problem of the predator-prey model, utilizing the Beddington DeAngelis functional response and incorporating the second condition of Cardan's method, played a crucial role in establishing a comprehensive stability analysis. This analysis is depicted in Figs. 2 and 3. The construction of these diagrams enabled us to conduct stability assessments for each value of K, corresponding to various ν values. Through this analysis, we arrived at the same conclusion as [1] concerning the case when $K = 120$. However, our study encompassed multiple scenarios for bifurcation within the system, contingent on different values of K. In all instances, it was evident that the presence of infochemicals had a stabilizing effect on what would otherwise be an unstable food web.

- By examining the behavior of the predator, denoted as M, and systematically varying the value of K as a secondary control parameter while keeping infochemicals as the primary parameter, we demonstrated the influence of DMS (dimethyl sulfide) on the predation of grazers. This analysis revealed that the populations of both species, namely phytoplankton and microzooplankton, can experience substantial simultaneous increases. This phenomenon is visually represented in Figs. 3(a), 3(b), 3(c), and 3(d).

- By investigating the growth rate of phytoplankton, we uncovered the following insights: A low growth rate results in diminished phytoplankton density, ultimately destabilizing the model, as depicted in Fig. 2(d). Conversely, a high potential growth rate enables heterotrophic protists to persist even during phases of elevated predation. However, this system is highly responsive to increases in fast-growing prey, and this heightened

responsiveness may explain the existence of a limit cycle within the dynamical system.

- We examined how the inclusion of a kinesis model within a predator-prey model utilizing the Beddington DeAngelis functional response influenced the system. Fig. (5) illustrates that the predator model remained largely unaffected by kinesis movement. In contrast, kinesis had a noticeable impact on the prey population. Specifically, kinesis movement played a role in preventing the extinction of the prey population over time.

- The prey population faces a rapid risk of extinction due to predation. Initially, without the kinesis model, the prey population exhibits better survival up to time 10. However, an opposite trend emerges over time, such as at time 20, where the prey population with the kinesis model displays improved survival compared to the scenario without it.

- The size of predator populations, whether with or without kinesis, remains essentially unchanged. In contrast, the prey population with kinesis experiences an initial decrease in population size. This indicates that initially, having kinesis is not advantageous for the prey population in that particular space. However, it becomes beneficial, and the population manages to survive when the prey population without kinesis starts to decline, as illustrated in Fig. 6.

- In the model we have constructed and analyzed in this study, the predator population exhibits spatial behavior characterized by traveling waves.

Acknowledgement

We thank the two anonymous referees for their very careful reading that improved the manuscript.

References

[1] T. AS Al-Karkhi, Rudy Kusdiantara, Hadi Susanto, Edward A Codling, *Bloom formation and turing patterns in an infochemical mediated multitrophic Plankton model*, International Journal of Bifurcation and Chaos, World Scientific, 30 (2020), 30-48.

[2] M. Kot, *Elements of mathematical ecology*, Cambridge University Press, (2001), 163-172.

[3] J. Huisman, Thi N.N.P, M.K. David, B. Sommeijer, *Reduced mixing generates oscillations and chaos in the oceanic deep chlorophyll maximum*, Nature 439, Nature Publishing Group, (2006), 32-325.

[4] A. Turing, *The chemical basis of morphogenesis*,Philosophical the Royal Biological Transactions Society Sciences, Phil. Trans. R. Soc. Lond. B, 237 (1952), 37-72

[5] S. V. Petrovskii, Horst Malchow, *A minimal model of pattern formation in a prey-predator system*, Elsevier, 29 (1999), 49-63.

[6] R. Nickalls, *A new approach to solving the cubic: Cardan's solution revealed*, The Mathematical Gazette, (1993), 354-359.

[7] S. M., H. FM., *The hydra effect in predator-prey models*, J. Math. Biol., Springer, 64 (2012), 341-360.

[8] A. M. Edwards, John Brindley, *Zooplankton mortality and the dynamical behaviour of plankton population models*, Bulletin of Mathematical Biology, Springer, 61 (1999), 303-339.

[9] P. JS Franks, *NPZ models of plankton dynamics: their construction, coupling to physics, and application,* Journal of Oceanography, Springer, 58 (2002), 379-387.

[10] A. Morozov, E. Arashkevich, A. Nikishina, K. Solovyev, *Nutrient-rich plankton communities stabilized via predator-prey interactions: revisiting the role of vertical heterogeneity*, Mathematical Medicine and Biology: Journal of the IMA, Oxford University Press, 28 (2010), 185-215.

[11] E. Saiz, c. Calbet, A. Albert, *Scaling of feeding in marine calanoid copepods*, Limnology and Oceanography, Wiley Online Library, (2007), 668-675.

[12] B. Hansen, T. KS, UC. Berggreen, *On the trophic fate of Phaeocystis pouchetii (Harlot). III. Functional responses in grazing demonstrated on juvenile stages of Calanus finmarchicus (Copepoda) fed diatoms and Phaeocystis*, Journal of Plankton Research, Oxford Univ Press, (1990), 1173-1187.

[13] A. M. Edwards, A. Yool, *The role of higher predation in plankton population models*, Journal of Plankton Research, Oxford Univ Press, (2000), 1085-1112.

[14] M. Jankovic, S. Petrovskii, *Are time delays always destabilizing? Revisiting the role of time delays and the Allee effect*, Theoretical Ecology, 7 (2014), 335-349.

[15] M. H. Cortez, Peter A. Abrams, *Hydra effects in stable communities and their implications for system dynamics*, Wiley Online Library, 97 (2016), 1135-1145.

[16] J. Harlim, W.F. Langford, *The cusp-Hopf bifurcation*, World Scientific, 17 (2007), 2547-2570.

[17] P. Davidson, *Post Keynesian macroeconomic theory*, Edward Elgar Publishing, (2011), 57-82.

[18] C. Robert, L. Thomas, I. Bondarenko, S. O'Day, J. Weber, C. Garbe, C. Lebbe, J. François Baurain, A. Testori, J. Jacques Grob, N. Davidson, J. Richards, M. Maio, A. Hauschild, W. H Miller Jr, P. Gascon, M. l Lotem, K. Harmankaya, R. Ibrahim, S. Francis, Tai-Tsang Chen, R. Humphrey, A. Hoos, J. D Wolchok others, *Ipilimumab plus dacarbazine for previously untreated metastatic melanoma*, Journal of New England Journal of Medicine, 364 (2011), 2517-2526.

[19] P. A. Abrams, C.I. J. Walters, *Invulnerable prey and the paradox of enrichment*, Journal of Ecology, Wiley Online Library, 77 (1996), 1125-1133.

[20] J.E. Truscott, J. Brindley, *Ocean plankton populations as excitable media*, Bulletin of Mathematical Biology, Elsevier, 56 (1994), 981-998.

[21] M. Haque, *A detailed study of the Beddington-DeAngelis predator-prey model*, Mathematical Biosciences, Elsevier, 234 (2011), 1-16.

[22] A.C. Alderkampa, M. Matthew, C.E. G. van Dijkena, L.A. Gerringac, H. J.W. deBaarb, C.D. Payned, R.J.W. Visserb, A.J. Bumab, K. R. Arrigo, *Iron from melting glaciers fuels phytoplankton blooms in the Amundsen Sea (Southern Ocean): Phytoplankton characteristics and productivity*, Deep Sea Research Part II: Topical Studies in Oceanography, Elsevier, 71 (2012), 32-48.

[23] M. Sieber, F. M. Hilker, *The hydra effect in predator-prey models*, Journal of Mathematical Biology, Springer, 64 (2012), 341-360.

[24] H. Song, R. Ji, C. Stock, K. Kearney, Z. Wang, *Interannual variability in phytoplankton blooms and plankton productivity over the Nova Scotian Shelf and in the Gulf of Maine*, Marine Ecology Progress Series, 426 (2011), 105-118.

[25] S. Sarwardi, Md. Reduanur Mandal, Nurul Huda Gazi, *Dynamical behaviour of an ecological system with Beddington-DeAngelis functional response*, Modeling Earth Systems and Environment, Springer, 2 (2016), 106-120.

[26] S. Shulin, G. Cuihua, *Dynamics of a beddington-DeAngelis type predator-prey model with impulsive effect*, Journal of Mathematics, Hindawi, (2013), 93-105.

[27] S. Jennings, M. Kaiser, J. D. Reynolds, *Biodiversity: an introduction,* Second Edition, Marine fisheries ecology, John wiley & Sons, (2009), 87-93.

[28] M. Steinke, G. Malin, P. S. Liss, *Trophic interactions in the sea: an ecological role for climate-relevant volatiles*, Journal of phycology, Wiley Online Library, 38 (2002), 630-638.

[29] J. Huisman, N.N. Pham Thi, D.M. Karl, B. Sommeijer, *Reduced mixing generates oscillations and chaos in the oceanic deep chlorophyll maximum*, Nature Publishing Group, 439 (2006), 322-329.

[30] A. Zagarts, A. Doleman, N.N. Phamthi, B.P. Sommeijer, *Blooming in a non-local, coupled phytoplankton nutrient model*, SIAM J. Appl. Math., 69 (2009), 1204-1174.

[31] A. Zagaris, A. Doleman, *Emergence of steady and oscillatory localized structures in a phytoplankton-nutrient model*, Nonlinearity, 24 (2011), 3437-348.

[32] E. Bard, *Nullclines and phaseplanes*, (2002), 123-131.

[33] W.C. Leggett a, E. Deblois, *Recruitment in marine fishes: is it regulated by starvation and predation in the egg and larval stages?*, Netherlands Journal of Sea Research, Elsevier, 32 (1994), 119-134.

[34] T. Caraco, H.R. Pulliam, *Sociality and survivorship in animals exposed to predation*, (1984), 34-48.

[35] C. Cosner, *Reaction-diffusion-advection models for the effects and evolution of dispersal*, Discrete Contin. Dyn. Syst., 34 (2014), 1701-1745.

[36] N. Gabukolu, *Impact of the purposeful kinesis on travelling waves,* Physica A: Statistical Mechanics and its Applications, 571 (2021), 125-821.

[37] P.C. Fife, *Lecture notes in biomathematics. In Mathematical Aspects of Reacting and Diffusing Systems*, Springer-Verlag Berlin, 28 (1979), 87-99.

[38] R.A. Fisher, *The genetical theory of natural selection: a complete variorum edition*, Oxford University Press, (1999), 67-74.

[39] C.L. Folt, *An experimental analysis of costs and benefits of zooplankton aggregation*, Predation, Direct and Indirecct Impacts on Aquatic Communities, (1987), 300-314.

[40] W.A. Foster, J.E. Treherne, *Evidence for the dilution effect in the selfish herd from fish predation on a marine insect*, Nature, 293 (5832), 466-474.

[41] A.N. Gorban, *Selection theorem for systems with inheritance*, Math. Model. Nat. Phenom., 4 (2007), 1-45.

[42] A.N. Gorban, N. Çabukoğlu, *Basic model of purposeful kinesis*, Ecological Complexity, 33 (2018), 75-83.

[43] A.N. Gorban, N.Çabukoğlu, *Mobility cost and degenerated diffusion in kinesis models*, Ecological Complexity, 36 (2018), 16-21.

[44] A.N. Gorban, M.G. Sadovskiy, *Optimal strategies of spatial distribution: the Allee effect*, Zh. Obshch, Biol., 50 (1989), 67-83.

[45] T. Hillen, K.J. Painter, *A users guide to PDE models for chemotaxis*, Journal Math. Biol, 58 (2009), 183-217.

[46] K.P. Hadeler, F. Rothe, *Travelling fronts in nonlinear diffusion equations*, Journal of Mathematical Biology, 3 (1975), 251-263.

[47] J.B.S. Haldane, *The causes of evolution*, Longmans Green, London, (1932), 32-41.

[48] E.F. Keller, Segel, L.A., *Model for chemotaxis*. J. Theor. Biol., 30 (1971), 225-234.

[49] R.E. Kenward, *Hawks, doves: factors affecting success and selection in goshawk attacks on woodpigeons*, The Journal of Animal Ecology, (1978), 449-460.

[50] A.N. Kolmogorov, I.G. Petrovsky, N.S. Piskunov, *Investigation of the equation of diffusion combined with increasing of the substance and its application to a biology problem*, Bull Moscow State Univ Ser A: Math and Mech, 6 (1937), 1-25

[51] H. Kruuk, Predators, *Anti-predator behaviour of the Black-headed Gull*, (Laurus Ridibundus L.), Brill Archive, 11 (1964), 56-71

[52] N.D. Lewis, M.N. Breckels, S.D. Archer, A. Morozov, J.W. Pitchford, M. Steinke, E.A. Codling, *Grazing-induced production of DMS can stabilize food-web dynamics and promote the formation of phytoplankton blooms in a multitrophic plankton model*, Biogeochemistry, 110 (2012), 303-313.

[53] M.A. Lewis, P. Kareiva, *Allee dynamics and the spread of invading organisms*, Theoretical Population Biology, 43 (1993), 141-158.

[54] J.A. Metz, R.M. Nisbet, S.A. Geritz, *How should we define fitness for general ecological scenarios?*, Trends. Ecol. Evol., 7 (1992), 198-202.

[55] A. Morozov, S. Petrovskii, B.L. Li, *Spatiotemporal complexity of patchy invasion in a predator-prey system with the Allee effect*, J. Theory. Biol., 238 (2006), 18-35.

[56] N.D. Solve, *Wolfram Language & System Documentation Center*, (2014), 78-87.

[57] G.A. Parker, J.M. Smith, *Optimality theory in evolutionary biology*, Nature, 348 (1990), 62-96.

[58] C. S. Patlak, *Random walk with persistence and external bias*, B. Math. Biophys., 15 (1953), 311-338.

[59] C. Pdepe, *Solve initial-boundary value problems for parabolic-elliptic PDEs in 1-D*, MatWorks Documentation, (2017), 36-41.

[60] S.V. Petrovskii, A.Y. Morozov, E. Venturino, *Allee effect makes possible patchy invasion in a predator-prey system*, Ecol. Lett, 5 (2002), 345-352.

[61] M. Ralls, P. Harvey, A. Lyles, *Inbreeding in natural populations of birds and mammals,* in Conservation Biology, (M. Soule Ed.), Sinauer Associates, Massachusetts, (1986), 35-56.

[62] A. Rosenblueth, N. Wiener, *Purposeful and non-purposeful behavior,* Philos. Sci., 17 (1950), 318-326.

[63] N. Shigesada, K. Kawasaki, E. Teramoto, *Traveling periodic waves in heterogeneous environments*, Theoretical Population Biology, 30 (1986), 143-160.

[64] J.G. Skellam, *Random dispersal in theoretical populations*, Biometrika, 38 (1951), 196-218.

[65] L. Sewalt, A. Doelman, H G E Meijer, V. R. äfer, A. Zagaris, *Tracking pattern evolution through extended center manifold reduction and singular perturbations*, Phys. D, Elsevier, (2015), 298-299.

[66] M. Soule, M. Gilpin, W. Conway, T. Foose, *The millenium ark: how long a voyage, how many staterooms, how many passengers?*, Zoo Biology, 5 (1986), 101-113.

[67] N.D. Lewis, M.N. Breckels, M. Steinke, E.A. Codling, *Role of infochemical mediated zooplankton grazing in a phytoplankton competition model*, Ecological complexity, Elsevier, 16 (2013), 41-50.

[68] P. Turchin, P. Kareiva, *Aggregation in Aphis varians: an effective strategy for reducing predation risk*, Ecology, 70 (1989), 1008-1016.

[69] V. Volpert, S. Petrovskii, *Reaction diffusion waves in biology*, Physics of life reviews, 6 (2009), 267-310.

[70] M. J. Way, C. J. Banks, *Intra-specific mechanisms in relation to the natural regulation of numbers of Aphis fabae Scop*, Annals of Applied Biology, 59 (1967), 189-205.

[71] M. J. Way, M. Cammell, *Aggregation behaviour in relation to food utilisation by aphids. In Animal populations in relation to their food resources*, A symposium of the British Ecological Society, Oxford and Edinburgh, Blackwell, (1969), 229-247.

Accepted: October 20, 2023